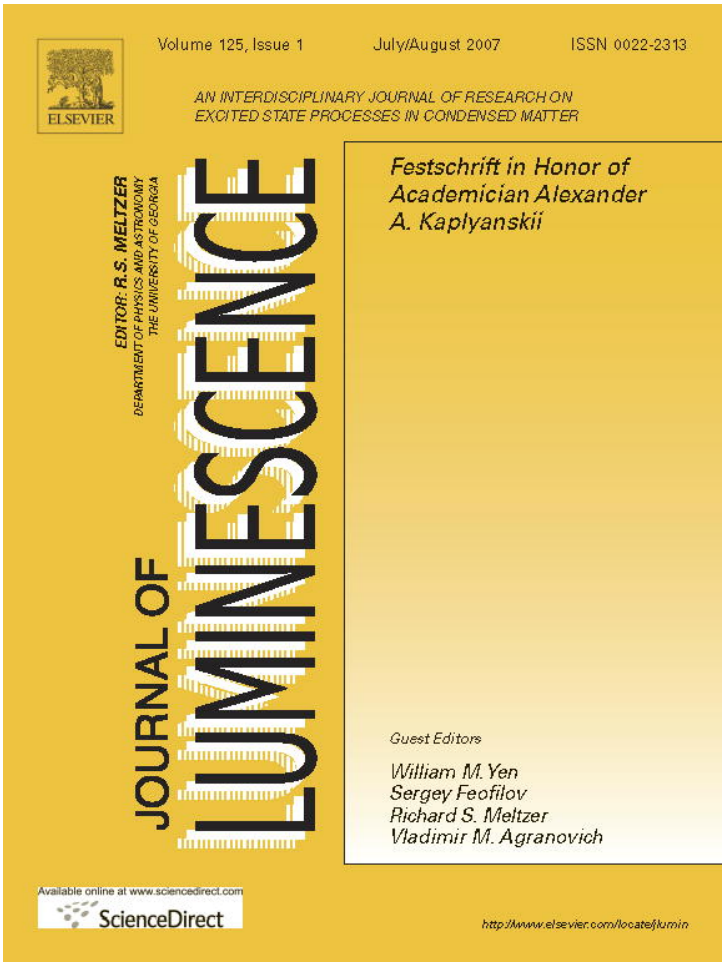

Available online at www.sciencedirect.com
ScienceDirect
Journal of Luminescence 125 (2007) 184–195
JOURNAL OF LUMINESCENCE
www.elsevier.com/locate/jlumin

En route to electrically pumped broadly tunable middle infrared lasers based on transition metal doped II–VI semiconductors

V.V. Fedorov, A. Gallian, I. Moskalev, S.B. Mirov*

Center for Optical Sensors and Spectroscopies, University of Alabama at Birmingham, Department of Physics, 1300 University Boulevard, Birmingham, AL 35294-1170, USA

Available online 22 September 2006

Abstract

In this work we report the study of Cr^{2+}:ZnSe photo-luminescence under UV and visible excitation as well as middle-infrared electroluminescence of n-type, Cr doped bulk ZnSe crystals. Photo-conductance studies were performed to verify $(2+)\rightarrow(1+)\rightarrow(2+)^*$ ionization transitions responsible for Cr^{2+} excitation. We report the first to our knowledge, Cr^{2+}:ZnSe lasing using 532 nm excitation. The first ever room temperature electroluminescence was also achieved in bulk n-type Cr:Al:ZnSe. This electroluminescence over 1800–2800 nm spectral range is in a good agreement with the mid-IR Cr^{2+} fluorescence under intra-shell optical excitation. Other spectral bands of electroluminescence were also observed at 600 nm and 8 μm. The visible electroluminescence observed is attributed to V_{zn}–Al complexes in conductive crystals. The nature of the 8 μm electroluminescence requires additional studies. Photo-ionization results are essential for optical pumping of Cr:ZnSe by easily available visible lasers, and, most importantly, both these and the electroluminescence results open a pathway for Cr:ZnSe broadband mid-IR lasing under direct injection of free carriers. Future directions for electrical excitation of low dimensional II–VI structures, where quantum confinement of the atomic impurity is used, could result in a much more efficient transfer of energy from the host to the localized impurity, are discussed.

PACS: 42.55.Rz; 42.55.Px; 71.20.Be; 71.20.Nr; 71.55.−I; 71.55.Gs; 78.30.Fs; 78.55.Et; 78.60.Fi

Keywords: Transition metal doped II–VI; Cr^{2+}:ZnSe; Photo-luminescence; Electroluminescence; Photo-conductance; Lasing

1. Introduction

There is a growing demand for affordable mid-infrared sources for use in a variety of applications including atmospheric sensing, eye-safe medical laser sources for non-invasive medical diagnostics, eye-safe laser radar and remote sensing of atmospheric constituents, optical communication, and numerous military applications. Recent research advances have spurred considerable effort in the development of practical mid-IR sources. This work has included direct generation in semiconductors using InAsSbP/InAsSb/InAs [1] and quantum cascade lasers [2–4]. Mid-IR wavelengths have also been generated using nonlinearities in optical parametric oscillators (OPOs) and difference frequency generators (DFGs) [5–7]. All of these approaches yield tunable sources in the mid-IR. However, all suffer some fundamental problems that limit their use as robust low-cost mid-IR source. OPOs and DFGs are expensive and bulky. Quantum cascade lasers are costly to manufacture, require low operating temperatures, and feature limited output power and range of tunability.

In parallel to the relatively large body of work using the approaches described above, there has been a significant effort on the direct mid-IR oscillation of crystals doped with rare-earth (RE) or transitional metal (TM) ions. Long wavelength RE and TM emissions are usually quenched by multi-phonon processes in conventional laser host media such as oxide and fluoride crystals, resulting in low room-temperature quantum efficiency of fluorescence.

Scientists from the Lawrence Livermore National Laboratory [10,11] were first to show that among all the

*Corresponding author. Tel.: +205 934 8088; fax: +205 934 8042.
E-mail address: mirov@uab.edu (S.B. Mirov).
URL: http://www.phy.uab.edu/~mirov/.

0022-2313/$ - see front matter © 2006 Elsevier B.V. All rights reserved.
doi:10.1016/j.jlumin.2006.08.010

solid state laser media TM^{2+} doped wide bandgap II–VI semiconductor crystals could be very special for mid-IR lasing. These TM^{2+} doped II–VI compounds have a wide bandgap and possess several important features that distinguish them from other oxide and fluoride laser crystals. These features are as follows:

- An important feature of the II–VI compounds is their tendency to crystallize as tetrahedrally coordinated structures, as opposed to the typical octahedral coordination at the dopant site. Tetrahedral coordination gives smaller crystal field splitting, placing the dopant transitions further into the IR.
- A key feature of these materials is that the heavy anions in the crystals provide a very low energy optical phonon cutoff that makes them transparent in a wide spectral region and decreases the efficiency of non-radiative decay, which gives a promise of a high yield of fluorescence at room temperature (RT). One can expect that in the column of anions from S, Se to Te the yield of RT fluorescence will increase.

Analysis of multiplet structure for low lying energy levels of V^{2+}, Cr^{2+}, Mn^{2+}, Fe^{2+}, Co^{2+}, Ni^{2+} in ZnSe and ZnS calculated by Fazzio et al. [8] and performed in Ref. [9] explains why the attention of researchers is mainly focused on Cr^{2+} and Fe^{2+} ions as the most promising dopants for effective broadly tunable lasing over 2–3 and 3.7–5 μm spectral regions, respectively.

- First excited levels of all considered ions except Mn^{2+} lie at the right energy to generate mid-IR emission.
- The ground and first excited levels of all the considered ions except Mn^{2+} have the same spin, and therefore will have a relatively high cross-section of emission.
- Higher lying levels of only two ions—Cr^{2+} and Fe^{2+}—have spins that are lower than the ground and first excited levels, greatly reducing the potential for significant excited state absorption at the pump or laser transition wavelengths.
- The orbital characteristics of the ground and first excited levels for Cr^{2+}, Fe^{2+} and Co^{2+} are different, and will experience a significant Franck–Condon shift between absorption and emission, resulting in broadband "dye-like" absorption and emission characteristics, suitable for a broadly tunable laser.

After pioneering publications [10,11], mid-IR laser activity near 2–5 μm has been reported for Cr^{2+}:ZnS [10–14], Cr^{2+}:ZnSe [10–22], Cr^{2+}:$Cd_{1-x}Mn_xTe$ [23], Cr^{2+}:CdSe [24], and Fe^{2+}:ZnSe [25] crystals. Recently we optimized technology for two-stage ZnS and ZnSe crystal preparation [12,13,26]. In the 1st stage, undoped single crystals were synthesized by a chemical transport reaction from gas phase using iodine gas transport scheme. During the 2nd stage, introduction of chromium and/or iron was performed by thermal diffusion from Cr or iron thin films deposited by pulsed laser deposition (PLD) method on a thin wafer of II–VI material. Several impressive results have been recently obtained with these new crystals:

(1) We developed the first continuous-wave RT tunable over more than 280 nm at ~2.3 μm Cr^{2+}:ZnS laser, pumped with a Co:MgF_2 laser and yielding over 100 mW of output power [27].
(2) Another key result is the first successful demonstration of CW Cr^{2+}:ZnS and ZnSe microchip lasers with the maximum output powers of 500 mW at 2320 nm and slope efficiency of 53% under direct (without coupling optics) Er-fiber laser excitation [26,28,31,32].
(3) We also developed the first gain switched Cr^{2+}:ZnSe microchip laser. A maximum slope efficiency of 6% and a maximum output energy of 1 mJ were obtained for a microchip without mirrors, when positive feedback was due only to the Fresnel reflections [28,32].
(4) First tunable directly diode-pumped, by the two conventional 500 mW InGaAsP–InP telecom laser diodes, version of CW Cr^{2+}:ZnS laser was also reported. Tunability over 400 nm between 2250 and 2650 nm was achieved [29,30].
(5) In an external cavity configuration a compact Er-fiber laser pumped broadly tunable over ~700 nm between 2170 and 2840 nm CW RT Cr^{2+}:ZnS laser was realized, yielding up to 700 mW at ~40% slope efficiency [31,32].
(6) First multiline and ultrabroadband lasing of Cr^{2+}:ZnSe in a spatially dispersive cavity has been realized [33].
(7) Finally, first RT gain-switched lasing of Fe:ZnSe was achieved in microchip and selective cavity configurations with tunability over 3.9–4.8 μm spectral range [34].

Current methods of pumping the chromium ion in Cr:ZnSe utilizes direct intra-shell excitation. However, electrically pumpable sources would be ideal for compact and portable lasers in the mid-IR. Electrically pumped mid-IR lasers based on TM doped II–VI structures have not been documented in the literature. Our hypothesis is that in addition to effective RT mid-IR lasing TM doped II–VI media, being wide band semiconductors, hold potential for direct electrical excitation. This work shows the initial steps towards achieving this goal by studying Cr^{2+} ion excitation into the upper laser state ^5E via photoionization transitions as well as via direct electrical excitation.

2. Excitation mechanisms of TM dopant ions in II–VI bulk semiconductors

2.1. Inter-band excitation of Cr^{2+} and Fe^{2+} in bulk II–VI semiconductors

For decades, the pure and doped (Cu and Mn) wide-bandgap II–VI semiconductors have been called promising

materials for the fabrication of light-emitting devices, and phosphors for electro-luminescent displays. It was noticed more than 50 years ago [35] that the inadvertent presence of TM ions such as chromium or iron provides very effective deactivation of visible light emission from donor–acceptor pair (DAP) or intra-shell transitions of Cu and Mn. Cr^{2+} and Fe^{2+} ions introduce deep energy levels in the forbidden gap, with $^5T_2$ being the ground state and ^5E the first excited state for chromium and vice versa for iron [36]. It was determined that in most of the chromium or iron-related recombination processes characteristic intra-center mid-IR emissions of Cr^{2+} and Fe^{2+} are induced ($^5E \rightarrow {}^5T_2$, with the wavelength $\sim 2\,\mu m$ for chromium and $^5T_2 \rightarrow {}^5E$, with the wavelength ~ 3.5–$5\,\mu m$ for iron) [37]. The nature of these processes of inter-band excitation and following Cr or Fe recombination can be quite different. It was found that mid-IR intra-shell PL of chromium and iron can be induced due to the following major processes depicted in Fig. 1.

(a) The first process relates to the binding of excitons by TM ions. For most of the cases excitons bound by TM ions decay nonradiatively and energy is transferred to states of the impurity, which was binding the exciton (Fig. 1a). So, the energy transfer results in intra-shell excitation $(TM^{2+})^*$ and not in ionization of a TM ion [38].
(b) The second process (see Fig. 1b) relates to TM excitation caused by energy transfer from an adjacent DAP to a TM ion leading to TM intra-shell excitation [39]. As in case (a) the energy transfer results in intra-shell excitation and not in ionization of the TM ion.
(c) The third process (see Fig. 1c) is due to TM^{2+} ionization caused by an Auger-type process, followed by recapture a hole or electron by the ionized TM and as in case (a) leads to mid-IR photo-luminescence (PL) [38,40].
(d) The fourth process (see Fig. 1d) relates to the fact that carrier trapping by ionized impurities can proceed through one of the highly excited states of the TM^{2+} impurity and thus result in intra-shell emission of TM ions [38,41].
(e) The fifth process is a direct excitation of the TM^{2+} centers in ZnSe by the impact of hot carriers. This mechanism is usually observed in Mn:ZnS thin film electroluminescent (TFEL) devices [42,49].
(f) Another possible mechanism of excitation suggests impact ionization of TM^{2+} [43].

The fourth process has been considered in details by Kimpel in Ref. [41]. Inter-band optical or electrical excitation generates electron–hole pairs

$$h\nu_g \rightarrow e^-_{CB} + e^+_{VB} \quad (1)$$

Electrons are captured by lattice neutral Cr^{2+} ions which then attain a quasi-negative charge state:

$$(Cr^{2+})^0 + e^-_{CB} + \rightarrow (Cr^{+})^- + h\nu_1 \quad (2)$$

The Cr^+ ion with negative effective charge would tend to attract the holes created in the reaction (1) with a subsequent formation of excited state Cr^{2+} according to reaction:

$$(Cr^{+})^- + e^+_{VB} \rightarrow (Cr^{2+})^* + h\nu_2 \quad (3)$$

and finally a radiative transition (mid-IR PL) to the ground state will close the cycle

$$(Cr^{2+})^* \rightarrow (Cr^{2+})^0 + h\nu_3 \quad (4)$$

Alternatively the free holes in the valence bands can be captured by Cr^{2+} impurities:

$$(Cr^{2+})^0 + e^+_{VB} \rightarrow (Cr^{3+})^+ + h\nu_4 \quad (5)$$

Conduction electrons would then recombine with these positively charged Cr^{3+} levels:

$$(Cr^{3+})^+ + e^-_{CB} \rightarrow (Cr^{2+})^* + h\nu_5 \quad (6)$$

Finally reaction (4) will take place leading to the mid-IR PL.

Processes similar to (5) and (6) have been successfully utilized by Klein in Ref. [44] where the first observation of laser oscillations at 3.53 μm due to intra-shell transitions of the Fe^{2+} centers in n-type InP:Fe under inter-band optical excitation was reported.

2.2. Optical sub-band (532 nm) excitation of Cr^{2+} in bulk II–VI semiconductors—excitation via photo-ionization transitions

The information discussed in the previous paragraphs clearly states that both chromium and iron belong to the most active centers of inter-band recombination leading to

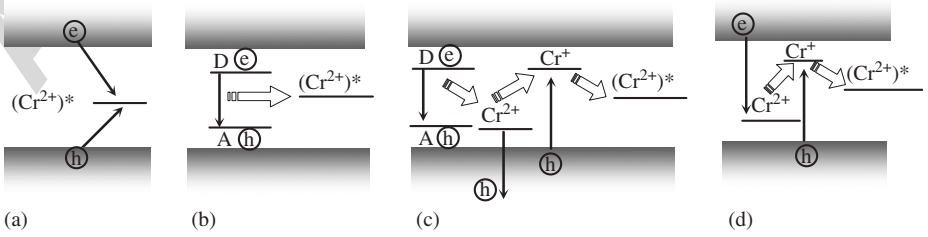

Fig. 1. Schematic diagram of major mechanisms of inter-band excitation of intra-shell mid-IR emission of Cr^{2+} and Fe^{2+} ions via (a) energy transfer from the bounded exciton; (b) energy transfer (ET) from adjacent DAP; (c) TM^{2+} ionization caused by a three center Auger-type recombination (TCAR) processes; (d) carrier trapping by ionized impurity.

intra-center excitation and mid-IR emission. It is of significant importance to study the nature of physical mechanisms of Cr^{2+} and Fe^{2+} ions optical inter-band excitation, to identify the most effective mechanisms and to formulate the conditions necessary for achieving mid-IR lasing. One of the objectives of this work was to study mechanisms and the efficiency of optical sub-band excitation of Cr^{2+} in ZnSe via photo-ionization transitions. These mechanisms are very similar to the processes of Cr^{2+} excitation via carrier's recombination and inter-band optical excitation. Understanding these mechanisms and achieving lasing of Cr^{2+} ions in ZnSe via its photo-ionization will be the first important step in demonstrating the feasibility of future Cr^{2+}:ZnSe mid-IR lasing under direct electrical excitation.

Photo-induced EPR studies of chromium doped ZnSe performed by Dr. Godlevski group [37–40,45] show that the Cr^{2+} center demonstrates an acceptor nature and under optical excitation with energy in excess of ~1.9 eV could release a hole in the valence band, with the Cr^{2+} being ionized into the Cr^{+} state. On the contrary, it has been shown that Cr^{+}, in spite of the fact that it is a good trap of holes, could be considered as a donor center. Indeed, under optical excitation with energy larger than ~0.8 eV Cr^{+} releases an electron in the conduction band forming $(Cr^{2+})^*$ in a highly excited state.

Fig. 2(a) and (b) depicts two possible processes of Cr^{2+} optical excitation via ionization transitions. As we have already discussed the Cr^{2+}/Cr^{+} level in ZnSe is located ~0.8 eV below the conduction and ~1.9 eV above the valence band of ZnSe, with a bandgap of ~2.7 eV. According to our notation of Fig. 2, energy of Cr^{2+} acceptor center "E_{ac}" is increased in the downward direction, while energy of the donor Cr^{+} center "E_d" is increased in the upward direction.

In the first process shown in Fig. 2(a) an incident photon with energy 2.33 eV (532 nm) ionizes the Cr^{2+} ion to the Cr^{+} state by releasing a hole to the valence band:

$$Cr^{2+} + h\nu \rightarrow Cr^{+} + e^{+}_{VB} \quad (7)$$

Subsequently a thermalized hole in the valence band is recombined with the Cr^{+} ion leading to formation of Cr^{2+} ion in a highly excited state $(Cr^{2+})^*$:

$$Cr^{+} + e^{+} \rightarrow (Cr^{2+})^* \quad (8)$$

Finally this state relaxes to the ^5E first excited energy level of Cr^{2+}, where radiative decay is accomplished by the emission of a mid-IR photon:

$$(Cr^{2+})^* \rightarrow (Cr^{2+}) + h\nu_{MIR} \quad (9)$$

The second route for Cr^{2+} excitation via photo-ionization transitions is depicted in Fig. 2(b). Initially, like in process (7), a 532 nm photon ionizes the Chromium ion from a 2+ state to a 1+ state with the generation of a hole in the valence band:

$$Cr^{2+} + h\nu \rightarrow Cr^{+} + e^{+}_{VB} \quad (10)$$

Next a second pump photon ionizes the chromium ion from a 1+ state to a 2+ excited state putting an electron in the conduction band:

$$Cr^{2+} + h\nu \rightarrow (Cr^{2+})^* + e^{-}_{CB} \quad (11)$$

The excited $(Cr^{2+})^*$, as in Eq. (9), relaxes to the ^5E first excited energy level of Cr^{2+}, which radiative decay is then accomplished by emission of mid-IR photon. As one can see, subsequent ionization of Cr^{2+} and Cr^{+} by two 532 nm quanta results not only in emission of an mid-IR quantum, but also in the electron-hole pair generation. Further recombination of the electron–hole pair could follow one of the routes of Fig. 1(b)–(d) resulting in $Cr^{2+}*$ emission of a second mid-IR photon.

3. Experimental verification of photo-ionization transitions

3.1. Photo-conductance

According to Fig. 2, 532 nm sub-band excitation of Cr^{2+} in ZnSe could lead to photo-ionization transitions (7–11) accompanied by formation of either a hole (Fig. 2(a) or an electron and hole carriers (Fig. 2(b)). Photo-conductance

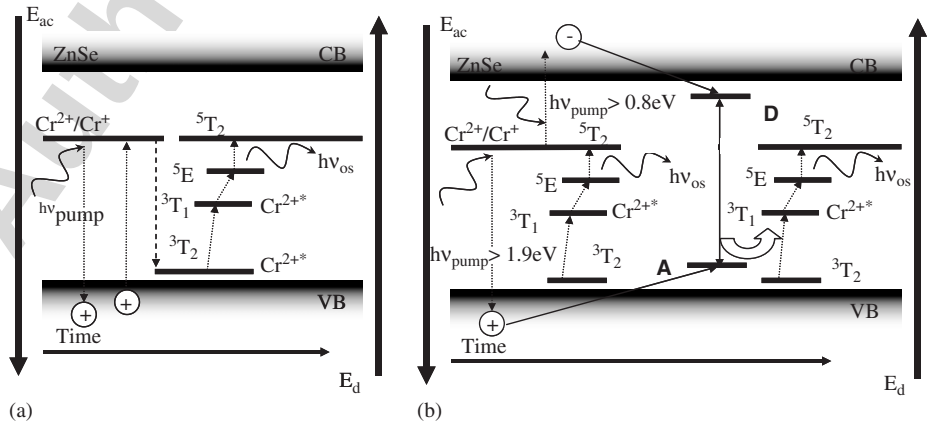

Fig. 2. Diagram of sub-band optical excitation of Cr^{2+} via ionization transitions: (a) Ionization through single photon interaction. (b) Multi-step ionization utilizing two pump photons and leading to the generation of two mid-IR photons.

measurements of bulk polycrystalline diffusion doped Cr^{2+}:ZnSe samples have been performed to verify photo-ionization mechanisms and show the existence of a photo-current under their 532 nm (2.33 eV) sub-band excitation.

Initial photo-conduction experiments were performed using a polycrystalline sample $1 \times 4 \times 8$ mm clamped between conducting layers of indium. The 2nd harmonic (532 nm) of a Nd:YAG laser was incident upon the long edge of the sample and a current was measured utilizing a load resistor of either 1 MΩ or 50 Ω.

Measurements of photo-current versus light intensity and bias voltage have been performed. Fig. 3 depicts a photo-current response of the system detected with a 50 Ω load. Comparison of the temporal shape of 532 nm excitation pulse (Fig. 3(I)) and photo-conductance voltage on the 50 Ω load resistor (Fig. 3(II)) show that the detected photo-current features a sub-nanosecond response time. This experiment demonstrates a fast relaxation (<1 ns) of photo-generated non-equilibrium carriers. Photo-current signal oscillation was due to the unbalanced impedance of the measurement system.

For the next experiments we used a square sample with side ≈ 4 mm and contacts on each corner. The contacts are made of indium and soldered to the sample and then the entire sample was heated. Finally the sample was chemically etched with ferric chloride to make the contacts as small as possible (sub 0.5 mm). These measurements were made with a Keithly 237 High Voltage Source Measurement Unit. Supplying a potential across 1–2 contacts and measuring the voltage drop across the two remaining corners (3,4) of the sample for different intensities of the 532 nm excitation shows interesting results (see Fig. 4). The curves show a monotonic response up to a threshold point. After this point the measured voltage drops significantly. After this drop the voltage appears to remain constant despite the applied potential in the forward (1–2) direction. This apparent change in resistance of the sample is caused by current spreading. Once a large enough current is generated the entire crystal conducts. Thus the potential difference between opposite sides is small. Of note is the fact that as the 532 nm radiation intensity is increased, this breakdown point shifts (see Fig. 4). As expected, as the incident 532 nm radiation power increases, the breakdown voltage decreases. This matches with the assumption that the change is due to current spreading, because as the illumination power increases the number of available carries also increases. This dependence of output signals on applied voltages and optical excitation could be of interest for optoelectronic applications.

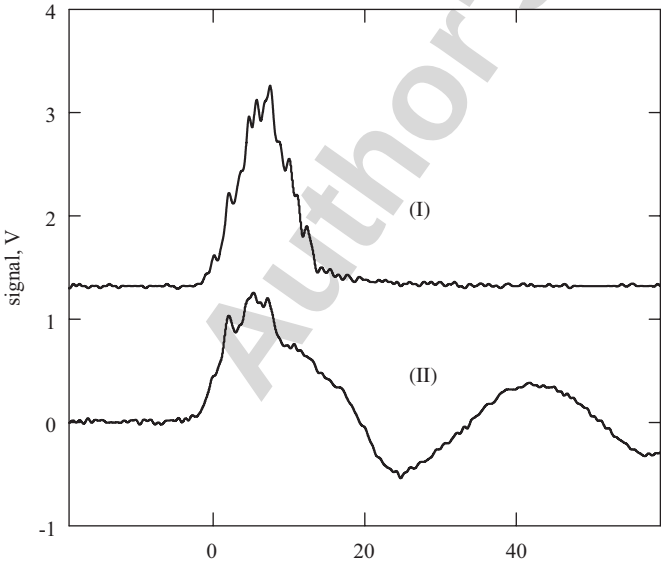

Fig. 3. Temporal shape of 532 nm excitation pulse (I) and photo-conductance voltage on the 50 Ω load resistor (II).

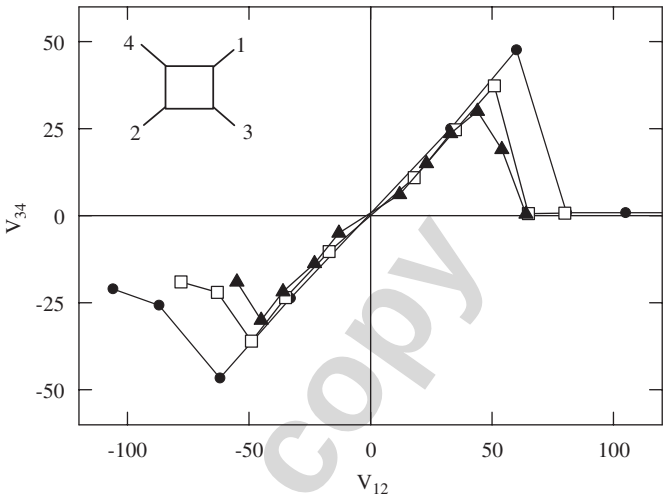

Fig. 4. Dependence of the potential difference across 3–4 contacts as a function of applied voltage in the forward 1–2 direction for variable intensity of 532 nm excitation. The voltage measured across the sample drops after a threshold level is reached in the forward (1–2) direction. This threshold level is reduced as the intensity of the 532 nm source is increased from triangles to filled circles.

To identify which of the mechanisms of Cr^{2+} photo-ionization is more preferable, photo-Hall voltage measurements were performed using a permanent magnet with a surface strength of ≈ 0.5 T and a 532 nm CW source. The sample was placed within 1 mm of the magnet and currents of up to 5 μA were applied. In this regime of applied current the accelerating voltage is above the breakdown threshold described in Fig. 4. This regime is believed to be the proper region so that a Hall voltage could be observed due to the existence of a current across the entire sample. Performed experiments show that the measured voltage polarities did not change with a change in the polarity of the magnetic field. It can be explained by an equal number of n- and p-type carriers generated under the 532 nm photo- excitation. This implies the mechanism of Cr ionization suggested in Fig. 2b could be accepted as the primary one.

3.2. Cr^{2+}:ZnSe mid-IR PL and lasing via photo-ionization transitions

In this work we experimentally verify Cr^{2+} excitation mechanisms of Figs. 1 and 2 by detecting mid-IR PL of Cr^{2+} ions under direct band-gap (355 nm) excitation of the ZnSe host as well as by detecting mid-IR PL and lasing of Cr^{2+} centers under sub-band 532 excitation via photo-ionization transitions. Similar charge transport phenomenon has been studied by Sorokina et al. in CVT and PVT grown samples [46,47] utilizing visible light to modulate the output power of directly pumped Cr^{2+} ions.

The polycrystalline samples were prepared from a 1 mm thick ZnSe optical window grown by chemical vapor transport, which was doped by thermal diffusion from a chromium thin film deposited by pulsed laser deposition. Thermal diffusion was performed in a sealed quartz ampoule at 10^{-5} Torr and a temperature of 1000 °C for 10 days. The PL studies were performed at 300 K under optical pumping by pulsed radiation 355, 532, or 1560 nm (~5 ns).

The time dependence of the mid-IR PL emission intensity is depicted in Fig. 5(i) and (ii), demonstrate a pump pulse profile and PL kinetics under intra-shell 1560 nm excitation with fast rise time and ~6 μs exponential decay. Fig. 5(iii) and (iv) are PL kinetics for 532 and 355 nm excitations, respectively, exhibiting a relatively slow growth (~3.5 μs) which reaches a peak at ~5 μs, and then decays with decay time of ~6 μs. Identical behavior of PL kinetics under UV and visible excitation indicates that they result from similar ionization mechanisms. This rise of the PL intensity for 532 and 355 nm excitations implies that ^5E population continues to grow long after the duration of the excitation laser pulse due to slow relaxation processes from higher-lying excited levels of Cr^{2+} to the upper laser level ^5E. At the same time the excited level is pumped at a rate faster than it is depleted and, hence it is reasonable to expect that the population of ^5E level could be inverted.

The laser set up consisted of a 3.5 mm thick uncoated plane-parallel 1×9 mm slab of polycrystalline Cr^{2+}:ZnSe and a hemispherical resonator formed with a gold mirror of radius 10 cm and a flat output coupler with reflectivity 95%. Pumping was achieved transversely with wavelength 532 nm from the second harmonic of a Nd:YAG Q-switched laser operated at 10 Hz with a pulse length of $\approx$5 nsec. Lasing of Cr^{2+}:ZnSe under 532 nm excitation was obtained and the temporal profiles of the lasing pulses are depicted in Fig. 5B(i) and B(ii) for 1560 and 532 nm excitations, respectively.

Further, evidence of lasing under 532 nm excitation is demonstrated in Fig. 6 showing a threshold dependence of the output input characteristics (Fig. 6A) and significant line narrowing of the emission spectrum (Fig. 6B).

3.3. Mid-IR electroluminescence of n-type bulk Cr^{2+}:ZnSe

As discussed in Refs. [42,43] luminescence can be electrically generated by impact excitation or ionization

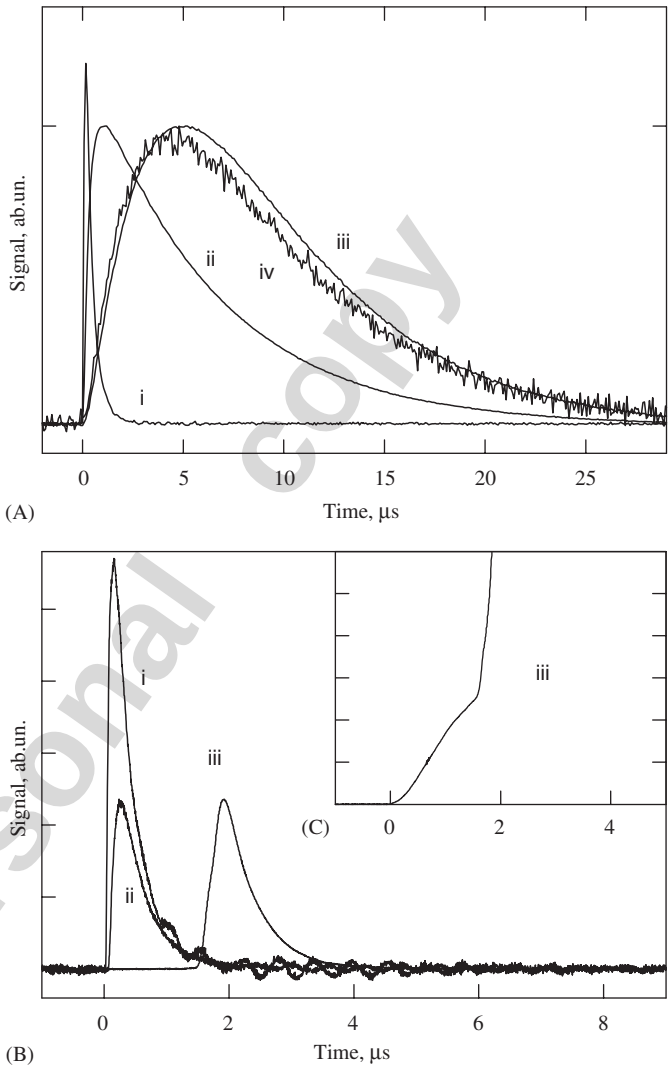

Fig. 5. (A) Kinetics of Cr:ZnSe single crystal mid-IR photo-luminescence at ~2500 nm under (ii) 1560 nm, (iii) 532 nm, (iv) 355 nm pumping with pump temporal profile shown in (i). (B) Dynamics of Cr:ZnSe laser oscillation build-up. Pulse (i) shows the pump pulse. Pulse (ii) shows the temporal profile of the lasing pulse from 1560 nm excitation. Pulse (iii) shows the temporal profile of the lasing pulse from 532 nm excitation. The inset (C) is a blow-up of the build-up part of the temporal profile of the 2500 nm lasing pulse under 532 nm excitation. This plot shows that ~2 μs build up time is required before mid-IR lasing occurs under 532 nm excitation.

of impurity levels in semiconductors. In Ref. [43] the first observation of mid-IR (~3500 nm) intra-center recombination radiation arising from impact ionization of Fe^{2+} impurities in thin (300 nm) layers of InP at cryogenic temperatures was reported. Conversion efficiency from injected electrical power to mid-IR optical power of $\sim 10^{-4}$% was obtained. This small value of conversion efficiency was explained due to the fact that only a small fraction of electrons in the tail of the population above the threshold level can impact ionize Fe^{2+}. There are also many publications on near IR emission in Si and SiO_x thin film electroluminescence (TFEL) based systems doped with Er Ref. [48]. TFEL devices based on mid-IR emitting ZnS

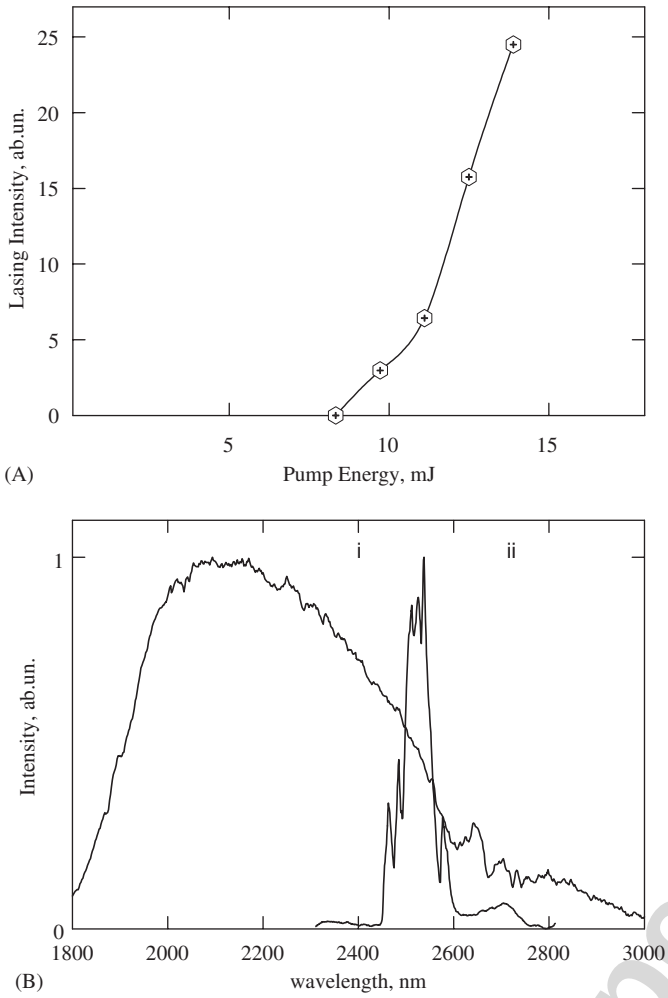

Fig. 6. (A) Lasing output versus pump energy incident upon the entire laser crystal. The threshold for lasing is ~7.5 mJ at 532 nm. (B) (i) PL spectrum of Cr:ZnSe polycrystalline sample under 532 nm excitation. (ii) The spectrum of Cr^{2+} lasing under 532 nm excitation.

(Se):Cr phosphors have been seldom investigated. In Ref. [49] the mid-IR electroluminescence in ZnS(Se):Cr electron beam evaporated thin films was first reported and the direct impact excitation of Cr^{2+} ions was identified as major mechanism of electroluminescence. One of the objectives of the current work was to obtain first room temperature mid-IR electroluminescence of bulk (~1 mm thick) n-type Cr^{2+}:ZnSe. We hypothesize that if mid-IR electroluminescence of bulk n-type Cr^{2+}:ZnSe would be detected, then much more efficient electroluminescence (and even lasing) of Cr^{2+} in p–n thin film and especially low dimensional structures could be envisioned.

3.3.1. Crystal preparation

The n-doped Cr:Al:ZnSe crystals were prepared using a two stage doping process. Pure ZnSe samples were grown using CVD and were doped by successive post-growth thermal diffusions of Cr and Al, respectively. The sizes of samples were about $1 \times 4 \times 4$ mm. During the first thermo-diffusion, the ZnSe samples were placed on top of Zn and CrSe powder and annealed in sealed evacuated ampoules (~10^{-5} Torr) for 7 days at 950 °C for crystal doping with active Cr^{2+} ions. Zinc powder was used in the annealing to prevent the formation of Zn vacancies, and CrSe was used to compensate for sublimation of Se.

The chromium concentration in the samples was evaluated using absorption measurements. After the chromium diffusion procedure the average absorption coefficient of Cr:ZnSe samples was about $k = 4\,\mathrm{cm}^{-1}$, which corresponds to a Cr^{2+} ions concentration of $N = 4 \times 10^{18}\,\mathrm{cm}^{-3}$.

The n-type samples were obtained by subsequent diffusion of Al impurities [50,51]. The crystals were placed on top of mixture of Zn and Al powders (97 wt% of Zn and 3 wt% of Al), and again placed in identical evacuated ampoules. They were annealed for 100 h at 950 °C. At the end of the aluminum annealing, the samples were quickly cooled by immersion in water. Subsequent thermo-diffusion of Al in Cr:ZnSe was accompanied by a ~two-fold decrease of the Cr^{2+} coefficient of absorption. However, Cr^{2+} absorption could still be observed. One of the reasons of the Cr^{2+} suppression could be compensation of divalent chromium by donor impurities in Cr:Al:ZnSe samples. Another reason relates to necessity to polish crystal faces after thermal diffusion of Al. Since the largest chromium concentration is near the surface of the crystal, the polishing might result in the removal of some amount of chromium dopant.

The emission spectra of $^5T_2 \leftrightarrow {}^5E$ transition of the Cr:ZnSe and Cr:Al:ZnSe samples under optical excitation were identical and in a good agreement with the published data [10,11,32,47].

3.3.2. Contacts formation and electrical properties

The procedure of formation of Ohmic contacts with indium as a contact material was performed as follows: in the beginning, the surfaces of the samples were slightly polished and cleaned to avoid surface conductivity effects. After drying, the crystal was heated to about 120 °C and liquid indium was applied to the facet of the crystal. Once the indium wet the surface and spread evenly over it, the crystals were placed on an uncoated side and heated to about 250 °C for several minutes. This heating allowed near-surface diffusion of indium necessary for proper contact formation [52].

The conductivity of the crystals was verified by I–V measurements in the 0–120 V range of potential differences across the sample with a series resistor of $R = 84.5\,\Omega$. To avoid self-induced overheating, the measurements were performed with a HP 214B pulse generator with a pulse duration of ~100 μs and repetition rate of 8 Hz. The I–V measurements demonstrated that before the aluminum doping procedure the Cr:ZnSe sample had a high resistivity $\rho > 10^{10}\,\Omega\,\mathrm{cm}$. In n-type Al–doped samples the dark resistivity at RT was decreased down to a value of $\rho = 10^2$–$10^4\,\Omega\,\mathrm{cm}$. The deviations in the samples conductivity were due to differences in the parameters of the

annealing process. The I–V characteristic of the Al–Cr:ZnSe crystal demonstrating the most intensive mid-IR electroluminescence is depicted in Fig. 7. As one can see from Fig. 7A, the I–V curve features quasi-Ohmic behavior with $R \approx 53\,\mathrm{k\Omega}$ ($\rho = 84\,\mathrm{k\Omega\,cm}$) for small ($<2\,\mathrm{V}$) voltages across the sample. However, as shown in Fig. 7B for voltages across the sample larger than 2 V the I–V curve feature nonlinear behavior with differential resistance of $R = 3.8\,\mathrm{k\Omega}$ for voltages of the order of 100 V. This behavior of the sample could not be explained by the simple heating of the sample during measurements. The sample heating should have result in the current growth at the end of the pulse. However, at low frequencies of operation of the pulse generator there were no changes in the temporal profile of the current through the sample for the whole range (up to 100 V) of applied voltages. One of the possible reasons of such behavior could be irregular contact formation on the facet of polycrystalline ZnSe sample. These irregularities could result in simultaneously pure Ohmic and Schottky behaviors for different parts of the sample. Another explanation of such behavior of the sample could be related to the formation of "conductive"

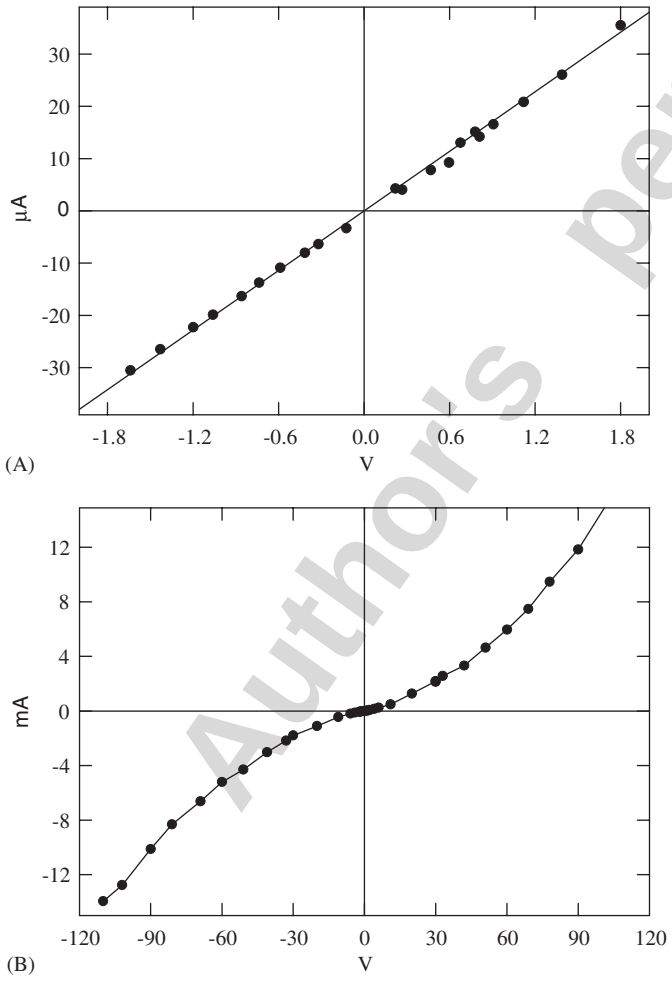

Fig. 7. Conductivity measurements of Cr:Al:ZnSe with In contacts for small (A) and large (B) potential differences across the sample.

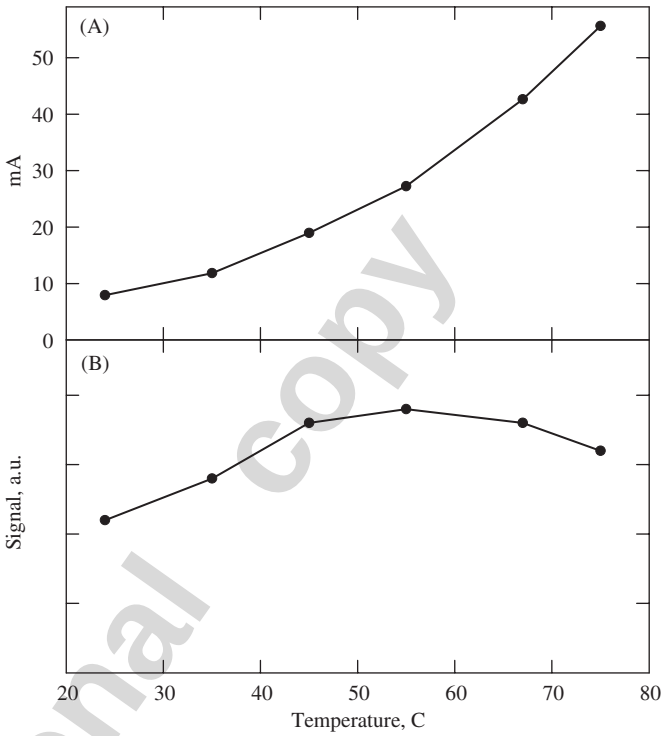

Fig. 8. Temperature dependences of the current through the sample (A) and the amplitude of the mid-IR electroluminescence (B).

channels through the sample at the stage of n-doping. In this case the nonlinear behavior of the I–V curve could be explained by a large current density in these channels. Fig. 8A shows a temperature dependence of the current through the sample. As one can see, sample heating till 70 °C results in a 7-fold decrease of the sample resistance with respect to the RT value.

3.3.3. Electroluminescence

Electroluminescence of the n-type Cr:Al:ZnSe samples was studied in the visible, near- and mid-IR spectral regions using photo-multiplier, InSb, and HgCdTe detectors. Excitation pulses with peak values up to 100 V and 19–70 μs duration were applied to the samples. Initially signal from electrically excited Cr:Al:ZnSe sample was detected without spectrometer with the use of a 2–3 μm bandpass filter and a InSb detector. Figs. 9 and 10 show the typical temporal profiles of the voltage across the sample (I) and the detected mid-IR optical signal (II). Optical signals were measured using a InSb detector with the time constant of the detector-preamplifier being ~0.5 μs. It is clear that the infrared signal observed in the 2–3 μm spectral range is due to electrical excitation, as it is perfectly in phase with the excitation pulses.

Fig. 8B demonstrates the dependence of the amplitude of the mid-IR electroluminescence versus temperature. In the range of temperatures from room to 55 °C the ascent of the intensity of the optical signal could be explained by the increase of the current amplitude, which happens due to the temperature dependent decrease of the sample

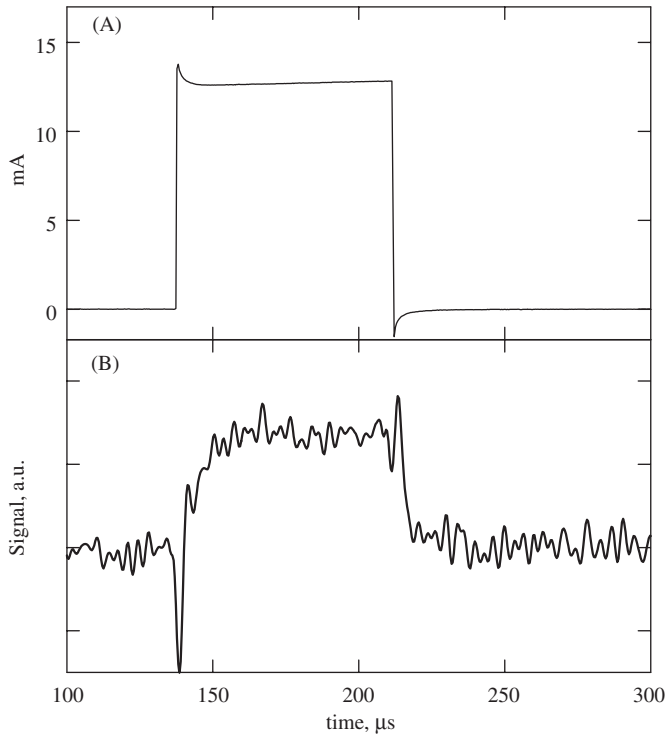

Fig. 9. The oscilloscope traces of the voltage across the sample (I) and the mid-IR optical signal (II).

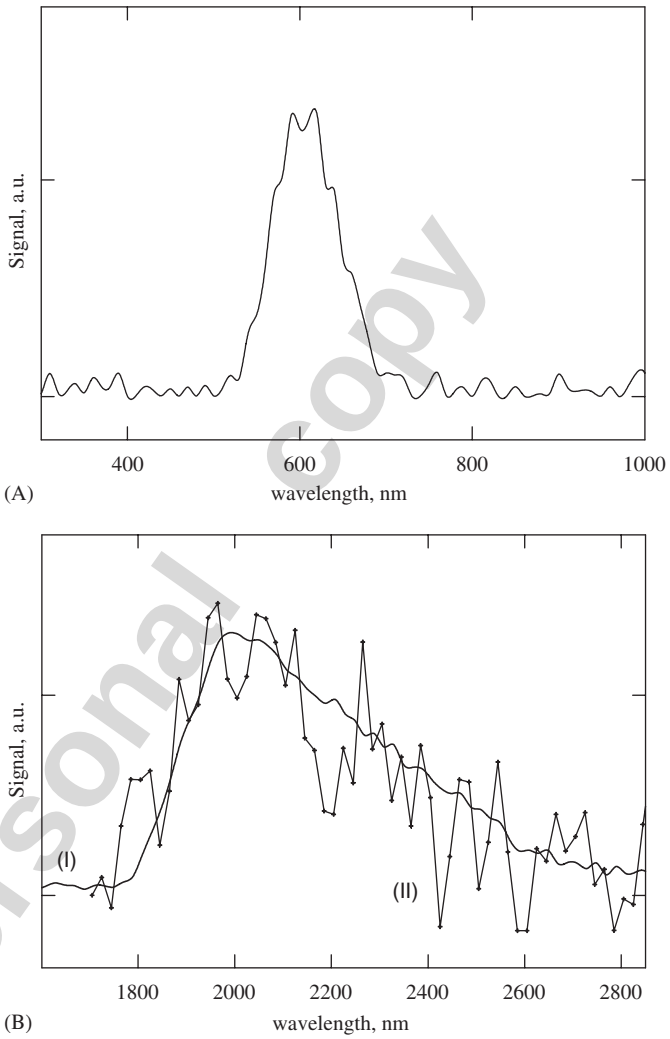

Fig. 10. Visible (A) and mid-IR (B) emission spectra of n-type Cr:Al:ZnSe under electrical (curve—II) and direct optical $^5T_2 \leftrightarrow {}^5E$ excitation (curve—I).

resistivity. The decrease in the intensity of the optical signal for temperatures above 55 °C is due to the temperature induced decrease of the Cr^{2+} quantum efficiency of luminescence.

The mid-IR electroluminescence spectrum of Cr:Al:ZnSe is depicted in Fig. 10B curve II. As one can clearly see the Cr:Al:ZnSe electroluminescence is in a good agreement with PL of the same sample measured under direct optical $^5T_2 \leftrightarrow {}^5E$ excitation (curve—II).

It was also revealed that under electrical excitation in addition to Cr^{2+} mid-IR electroluminescence there exist luminescence signals in two other spectral bands. Fig. 10A demonstrates a strong visible emission band detected near 600 nm. It was visible even with the naked eye. Some authors assign this emission to V_{Zn}–Al complex in conductive crystals [50].

In addition to these bands the luminescence band around 8 μm was also observed under electrical excitation. The nature of the 8 μm electroluminescence is not yet understood at this time.

4. Future directions

4.1. Inter-band and intra-shell excitation of Cr^{2+} and Fe^{2+} in low-dimensional II–VI structures

There are numerous publications related to preparation, luminescence properties and potential applications of Mn^{2+}:II–VI nanoparticles. The interest to this phosphor was stimulated by Bhargava [53] whose most fundamentally interesting result was luminescence enhancement resulting from efficient energy transfer from the ZnS nanocrystals to Mn^{2+} ions facilitated by mixed electronic states. Regarding Cr and Fe doped II–VI nanocrystals their photo–physical properties have not yet been addressed. It is believed that similarly to Mn doped ZnS nanocrystals, one can expect an efficient energy transfer from the low dimensional II–VI structures to Cr^{2+} and Fe^{2+}. Fast energy transfer from the low-dimensional host to Cr^{2+} and Fe^{2+} can be qualitatively explained by the increase of the exciton oscillator strength bound to the impurity center. First of all, quantum size confinement should increase the oscillator strength of the free exciton due to an increase of the electron–hole overlap factor. Secondly, the oscillator strength of the exciton bounded to the impurity center depends on the oscillator strength of the free exciton and electron–hole exchange interaction term which is also supposed to be large due to the carrier's confinement. Thus, we may expect a large enhancement of the oscillator strength of the exciton bound to the impurity embedded in

nanostructured materials with respect to bulk hosts. Another important issue that was successfully proven by Tanaka [54] for Mn doped II–VI nanocrystals relates to remarkable differences in thermal quenching of TM d–d PL in nanocrystals and bulk materials. First of all, the density of states for both electron and phonons decreases with size. This is likely to result in weaker electron–phonon coupling opening a pathway for development of a mid-IR light emitting nanostructured material with high RT quantum efficiency of PL under intra-shell IR optical excitation. Hence, Fe^{2+} doped bulk II–VI lasers can operate efficiently only at liquid nitrogen temperature (LNT), whereas Fe^{2+} doped nanostructured materials might lase at RT. On the other hand, the increased overlap between the electron and hole wave functions decreases the exciton–phonon coupling. Analogously to Mn in ZnS, such nanostructured materials are supposed to provide much weaker thermal quenching of Fe^{2+} in nanocrystals than that of the bulk crystals. This analysis provides a background for the remarkable differences that could be expected in excitation of Cr^{2+} and Fe^{2+} ions in nanostructures with respect to the bulk crystals and thus the motivation for studies of these nanostructures.

We envision two promising roots for achieving TM^{2+}:II–VI mid-IR lasing under electrical excitation.

4.2. Electrical excitation of II–VI nanocrystals co-activated by transition metals and dispersed in a conductive matrix

Recently, chemically synthesized semiconductor nanoparticles attracted much attention as a potential easily tunable optically and electrically pumpable gain media. First demonstration of an optically pumped semiconductor nanocrystal laser was given by Klimov's group at LANL [55]. Electrically pumped room-temperature lasing from a CdSe quantum dot stack separated by ZnSSe spacer layers of high S content has been reported at a wavelength around 560.5 nm with threshold current density of 7.5 kA/cm^2 [56]. Klimov et al. in [55] determined the required material and optical parameters to realize gain in close packed films of semiconductor nanocrystals. Good surface passivation, narrow size distribution, low re-absorption by the host material at the lasing frequencies, and high (>0.002) volume fraction of nanoparticles in the host material are the major issues for achieving stimulated emission. The approach of *utilization of II–VI nanocrystals co-activated by TM and dispersed in a conductive matrix for achieving mid-IR lasing under direct electrical excitation* is based on three innovative ideas combined in one system. The first key element of the system utilizes above mentioned principles of electrical excitation of closed pack films of undoped nanocrystals [55] and light emitting diodes (LEDs) designed [57] using semiconductor nanocrystallites (quantum dots) dispersed in a matrix. Using this approach Alivisatos [57] produced LEDs with high conversion efficiencies by utilizing quantum dots embedded in polymer matrices. *The second key element* relates to the fact that although nanocrystallites have not yet completed their evolution into bulk solids, structural studies indicate that they have the bulk crystal structure and lattice parameter [58]. This fact provides a strong foundation for our hypothesis that similar to the bulk II–VI crystals, tetrahedral coordination of TM^{2+} centers in II–VI nanocrystallites will provide a small crystal field splitting and place the dopant transitions into the mid-IR. *The third key element* of the system utilizes the "quantum-confined atoms" approach proposed recently by Bhargava [59]. Because the radii of the excited states of an impurity (0.1–1 nm) are significantly smaller than the typical Bohr radii of exciton in semiconductors (3–10 nm) the wavelength of the impurity characteristic fluorescence should hardly change, whereas the spectroscopic characteristics such as oscillator strength and intensity of the mid-IR transition can be modulated by quantum confinement. The most interesting results, in the case of the quantum confined impurity, are an efficient energy transfer from the host nanocrystal to the impurity accompanied by the relaxation of the selection rules for intra-shell transitions of TM^{2+} ions and corresponding fluorescence enhancement, which was verified for ZnS:Mn^{2+} nanocrystals by several authors [60,61].

This is a very attractive approach, especially if combined with simultaneous confinement of carriers and photons, which provides smaller threshold and larger output power.

4.3. Electrical excitation of doped II–VI heterostructures

For decades, the wide-band-gap II–VI semiconductors, particularly ZnSe, have been called promising materials for the fabrication of *visible* LEDs and lasers. The lifetime of II–VI based LEDs already exceeds 10,000 h [62]. We believe that utilization of II–VI heterostructures with active layer co-activated by transition metals is a promising route for achieving broadly tunable *mid-IR* lasing under direct electrical excitation. The structure of the lasers could be similar to double heterojunction blue-green lasers based on a ZnMgSSe alloy forming a type I heterostructure with ZnCdSe [63,64], where the active ZnCdSe layer is doped by Cr^{2+} or Fe^{2+} ions. The layer should be QW or QD and in addition to simultaneous confinement of carriers and photons the effective (due to phenomena of quantum confinement) energy transfer from the host to the emitting ion is provided.

5. Conclusions

We demonstrated clear evidence of Cr:ZnSe lasing at 2.4 μm induced by $2+ \rightarrow 1+ \rightarrow 2+$ ionization transitions of chromium ions. The semiconductor nature of the ZnSe plays an important role in the Cr^{2+} pumping, occurring via Cr^{+} created during the exciting pulse putting a hole into the valence band and subsequent ionization to the Cr^{2+} excited state. Later recombination of the hole in the valence band from the first photon, and the electron in the

conduction band from the second photon lead to energy transfer to the Cr^{2+} impurity. The generation of free carriers by photo-ionization of the Cr^{2+} ion was shown through the generation of a photo-current using illumination of the crystal with photons of lower energy than the bandgap of the host. Photo-Hall measurements tend to imply that the second proposed route of luminescence under 532 nm excitation is indeed correct.

Room temperature electroluminescence was achieved in n-type Cr:Al:ZnSe. Visible and mid-IR emissions were observed under electrical excitation. The mid-IR electroluminescence over the 1800–2800 nm spectral range is in a good agreement with Cr^{2+} fluorescence under optical excitation. The visible emission observed is in the 600 nm range and is attributed to V_{Zn}-Al complex in conductive crystals. The nature of 8 μm luminescence requires additional studies. Utilization of p–n junction structures should increase efficiency of the energy transfer from the host to Cr^{2+} ions.

Acknowledgements

This material is based upon work supported by the National Science Foundation under Grants no. ECS-0424310, EPS-0447675, and BES-0521036. We also acknowledge support from the Nation Science Foundation (NSF)-Research Experience (REU)-site award to the University of Alabama at Birmingham (UAB) under Grant no. DMR-0243640. We appreciate the technical assistance of Mr. Lawrence Luke.

References

[1] C. Sirtori, J. Faist, F. Capasso, D.L. Sivco, A.L. Hutchinson, A.Y. Cho, IEEE Photon. Technol. Lett. 9 (1997) 294.
[2] Y.H. Zhang, Appl. Phys. Lett. 66 (1995) 118.
[3] F. Capasso, et al., IEEE J. Select. Topics Quant. Elect. 6 (2001) 931 and references therein.
[4] R. Colombelli, et al., Appl. Phys. Lett. 78 (2001) 2620.
[5] K.S. Abedin, S. Haidar, Y. Konno, C. Takyu, H. Ito, Appl. Opt. 37 (1998) 1642.
[6] S.B. Mirov, A.O. Okorogu, W. Lee, D.I. Crouthamel, N.W. Jenkins, K.Graham, A.R. Gallian, A. Yu. Dergachev, W.B. Yan, W.J. Strachan, T.F. Steckroat, D.F. Heller, J.C. Walling, (July 1998) All solid state laser system, continuously tunable over 0.2–10 micron spectral range, in: G.A. Lampropoulos, R.A. Lessard, (Eds.), Applications of Photonics Technology 3: Closing the gap between Theory, Development, and Application, Procedings of SPIE, vol. 3491, July 1998, pp. 1082–1088.
[7] A.O. Okorogu, S.B. Mirov, W. Lee, D.I. Crouthamel, N. Jenkins, A.Yu. Dergachev, K.L. Vodopyanov, V.V. Badikov, Opt. Commun. 155 (1998) 307.
[8] A. Fazzio, M.J. Caldas, A. Zunger, Phys. Rev. B 30 (1984) 3430.
[9] W.F. Krupke, Adv. Lasers Appl., in: D.M. Finlayson, B.D. Sinclair (Eds.), Proceedings of the fifty second Scottish Universities Summer School in Physics, September 1998, SUSSP Publications & Institute of Physics Publishing, 1999.
[10] L.D. DeLoach, R.H. Page, G.D. Wilke, S.A. Payne, W.F. Krupke, IEEE J. Quantum Electron. 32 (1996) 885.
[11] R.H. Page, K.I. Schaffers, L.D. DeLoach, G.D. Wilke, F.D. Patel, J.B. Tassano, S.A. Payne, W.F. Krupke, K.T. Chen, A. Burger, IEEE J. Quantum Electron. 33/4 (1997) 609.
[12] K. Graham, S.B. Mirov, V.V. Fedorov, M.E. Zvanut, A. Avanesov, V. Badikov, B. Ignat'ev, V. Panutin, G. Shevirdyaeva, Spectroscopic characterization and laser performance of diffusion doped Cr^{2+}:ZnS, in: S. Payne, C. Marshall (Eds.), OSA Trends in Optics and Photonics on Advanced Solid State Lasers, vol. 46, Optical Society of America, Washington, DC, 2001, pp. 561–567.
[13] K. Graham, S.B. Mirov, V.V. Fedorov, M.E. Zvanut, A. Avanesov, V. Badikov, B. Ignat'ev, V. Panutin, G. Shevirdyaeva, Spectroscopic characterization and laser performance of diffusion doped Cr^{2+}:ZnS, in: L. Marshall (Ed.), Advanced Solid State Lasers, OSA Technical Digest, Optical Society of America, Washington, DC, 2001, pp. WB12-1–WB12-3.
[14] K. Graham, S. Mirov, V. Fedorov, M.E. Zvanut, A. Avanesov, V. Badikov, B. Ignat'ev, V. Panutin, G. Shevirdyaeva, Laser performance of Cr^{2+} doped ZnS, in Solid State Lasers X, in: R. Scheps, (Ed.), Proceedings of SPIE, vol. 4267, 2001, pp. 81–88.
[15] G.J. Wagner, T.J. Carrig, R.H. Page, K.I. Schaffers, J.O. Ndap, X. Ma, A. Burger, Opt. Lett. 24 (1999) 19.
[16] O. Podlipensky, V.G. Shcherbitsky, N.V. Kuleshov, V.I. Levchenko, V.N. Yakimovich, A. Diening, M. Mond, S. Kuck, G. Huber, 1 W continuous-wave laser generation and excited state absorption measurements in Cr^{2+}:ZnSe, in: H. Injeyan, U. Keller, C. Marshall (Eds.), OSA Trends in Optics and Photonics, Advanced Solid State Lasers, vol. 34, Optical Society of America, Washington, DC, 2000, pp. 201–206.
[17] I.T. Sorokina, E. Sorokin, A.D. Lieto, M. Tonelli, R.H. Page, K.I. Schaffers, 0.5 W efficient broadly tunable continuous-wave Cr^{2+}:ZnSe laser,, in: H. Injeyan, U. Keller, C. Marshall (Eds.), OSA Trends in Optics and Photonics, Advanced Solid State Lasers, vol. 34, Optical Society of America, Washington, DC, 2000, pp. 188–193.
[18] A. Sennaroglu, A.O. Konea, C.R. Pollock, Power performance of a continuous-wave Cr^{2+}:ZnSe laser at 2.47 μm, in: H. Injeyan, U. Keller, C. Marshall (Eds.), OSA Trends in Optics and Photonics, Advanced Solid State Lasers, vol. 34, Optical Society of America, Washington, DC, 2000, pp. 240–245.
[19] T.J. Carrig, G.J. Wagner, A. Sennaroglu, J.Y. Jeong, C.R. Pollock, Acousto-optic mode-locking of a Cr^{2+}:ZnSe laser, in: H. Injeyan, U. Keller, C. Marshall (Eds.), OSA Trends in Optics and Photonics, Advanced Solid State Lasers, vol. 34, Optical Society of America, Washington, DC, 2000, pp. 182–187.
[20] G.J. Wagner, T.J. Carrig, Power scaling of Cr^{2+}:ZnSe lasers, in: C. Marshall (Ed.), OSA Trends in Optics and Photonics, Advanced Solid State Lasers, vol. 50, Optical Society of America, Washington, DC, 2001, pp. 506–510.
[21] A.V. Podlipensky, V.G. Shcherbitsky, N.V. Kuleshov, V.I. Levchenko, V.N. Yakimovich, M. Mond, E. Heumann, G. Huber, H. Kretschmann, S. Kuck, Appl. Phys. B 72 (2001) 253.
[22] E. Sorokin, I.T. Sorokina, Room-temperature CW Diode-pumped Cr^{2+}:ZnSe Laser, in Advanced Solid State Lasers, OSA Technical Digest, Optical Society of America, Washington, DC, 2001, pp. MB11-1–MB11-3.
[23] U. Hommerich, X. Wu, V.R. Davis, S.B. Trivedi, K. Grasza, R.J. Chen, S. Kutcher, Opt. Lett. 22 (1997) 1180.
[24] J. McKay, D. Kraus, K.L. Schepler, Optimization of Cr^{2+}:CdSe for Efficient laser Operation, in: H. Injeyan, U. Keller, C. Marshall (Eds.), OSA Trends In Optics and Photonics, Advanced Solid State Lasers, vol. 34, Optical Society of America, Washington, DC, 2000, pp. 219–224.
[25] J.J. Adams, C. Bibeau, S.A. Payne, R.H. Page, Tunable laser action at 4.0 microns from Fe:ZnSe, in Advanced Solid State Lasers, OSA Technical Digest, Optical Society of America, Washington, DC, 2001.
[26] S.B. Mirov, V.V. Fedorov, K. Graham, I.S. Moskalev, V.V. Badikov, V. Panutin, Mid-IR Cr^{2+}:ZnS and ZnSe microchip lasers, in:

M.E. Fermann, L.R. Marshall (Eds.), Advanced Solid State Lasers, Optical Society of America, Washington, DC, 2002, pp. 364–370.
[27] I.T. Sorokina, E. Sorokin, S.B. Mirov, V.V. Fedorov, V. Badikov, V. Panyutin, A. DiLieto, M. Tonelli, Appl. Phys. B 74 (2002) 607.
[28] S.B. Mirov, V.V. Fedorov, K. Graham, I.S. Moskalev, V.V. Badikov, V. Panutin, CW and pulsed Cr^{2+}:ZnS and ZnSe microchip lasers, in OSA Trends in Optics and Photonics (TOPS) Conference on Lasers and Electro-Optics, OSA Technical Digest, Postconference Edition, vol. 73, OSA, Washington, DC, 2002, pp. 120-121.
[29] I.T. Sorokina, E. Sorokin, S.B. Mirov, V.V. Fedorov, V. Badikov, V. Panyutin, K. Schaffers, Opt. Lett. 27 (2002) 1040.
[30] I.T. Sorokina, E. Sorokin, S. Mirov, V. Fedorov, V.V. Badikov, V. Panutin, Broadly Tunable Continuous-Wave Cr^{2+}:ZnS Laser, in OSA Trends in Optics and Photonics (TOPS) Conference on Lasers and Electro-Optics, OSA Technical Digest, Postconference Edition, vol. 73, OSA, Washington, DC, 2002, pp. 118–119.
[31] S.B. Mirov, V.V. Fedorov, K. Graham, I.S. Moskalev, V.V. Badikov, V. Panyutin, Opt. Lett. 27 (11) (2002) 909.
[32] S.B. Mirov, V.V. Fedorov, K. Graham, I.S. Moskalev, I.T. Sorokina, E. Sorokin, V. Gapontsev, D. Gapontsev, V.V. Badikov, V. Panyutin, IEE Optoelectron. 150 (4) (2003) 340–345.
[33] I.S. Moskalev, S.B. Mirov, V.V. Fedorov, Opt. Express 12 (2004) 4986.
[34] J. Kernal, V.V. Fedorov, A. Gallian, S.B. Mirov, V.V. Badikov, Opt. Express 13 (26) (2005) 10608.
[35] N. Riehl, H. Ortman, Z. Phys. Chem. A 109 (1941).
[36] G. Grebe, H.J. Schulz, Z. Naturforsch. 29a (1974) 1803.
[37] A. Zakrzewski, M. Godlewski, J. Appl. Phys. 67 (5) (1990) 2457.
[38] M. Godlewski, A.J. Zakrzewski, V.Yu. Ivanov, J. Alloys Compd. 300–301 (2000) 23.
[39] M. Surma, M. Godlewski, Radiat. Effects Defects Solids 135 (1995) 213.
[40] M. Godlewski, M. Kaminska, J. Phys. C: Solid State Phys. 13 (1980) 6537.
[41] B.M. Kimpel, K. Lobe, H.J. Schulz, E. Zeitler, Measure. Sci. Technol. 6 (9) (1995) 1383.
[42] G.O. Muller, in: A.H. Kitai (Ed.), Solid State Lumin., Chapman & Hall, London, 1993, p. 138.
[43] G. Scamarcio, F. Capasso, A.L. Hutchinson, T. Tanbun-Ek, J. Appl. Phys. Lett. 68 (1996) 1374.
[44] P.B. Kleinm, J.E. Furneaux, R.L. Henry, Appl. Phys. Lett. 42 (8) (1983) 638.
[45] V.Yu. Ivanov, T.P. Surkova, M. Godlewski, N. Zhavoronkov, A.R. Omelchuk, Phys. Stat. Sol. (b) 229 (1) (2002) 355.
[46] T. Sorokina, E. Sorokin, Sensitization of the induced radiation in Cr^{2+}:ZnSe and Cr^{2+}:ZnS lasers, in OSA Trends in Optics and Photonics (TOPS) paper WB7 Nonlinear Optics Conference, vol. 79, Wailea, Maui, 2002, pp. 167–169 .
[47] T. Sorokina, Opt. Mater. 26 (2004) 395.
[48] M. Sopinsky, V. Khomchenko, Curr. Opin. Solid State Mater. Sci. 7 (2003) 97.
[49] N.A. Vlasenko, Z.L. Denisova, Ya.F. Kononets, L.I. Veligura, Yi.A. Tsyrkunov, J. Soc. Inform. Display 12 (2004) 179.
[50] J.C. Bouley, P. Blanconnier, A. Herman, Ph. Ged, P. Henoc, J.P. Noblanc, J. Appl. Phys. 46 (1975) 3549.
[51] V.A. Kasiyan, R.Z. Shneck, Z.M. Dashevsky, S.R. Rotman, Phys. Stat. Sol. (b) 229 (2002) 395.
[52] R. Kaufman, P. Dowbor, J. Appl. Phys. 45 (1974) 4487.
[53] R.N. Bhargava, D. Gallagher, X. Hong, A. Nurmikko, Phys. Rev. Lett. 72 (3) (1994) 416.
[54] M. Tanaka, J. Lumin. 100 (2002) 163.
[55] V.I. Klimov, A.A. Mikhailovsky, Su. Xu, A. Malko, J.A. Hollingsworth, C.A. Leatherdale, H.J. Eisler, M.G. Bawendi, Science 290 (2000) 314.
[56] M. Klude, T. Passow, R. Kroger, D. Hommel, Electron. Lett. 3 (2001) 1119.
[57] A.P. Alivisatos, Science 271 (1996) 933.
[58] C.B. Murray, D.J. Norrix, M.G. Bawendi, J. Am. Chem. Soc. 115 (1993) 8706.
[59] R.N. Bhargava, J. Cryst. Growth 214/215 (2000) 926.
[60] B.A. Smith, J.Z. Zhang, A.J. Joly, J. Liu, Phys. Rev. B 62 (2000) 2021.
[61] W. Chen, R. Sammynaiken, Y. Huang, J. Appl. Phys. 88 (2000) 5188.
[62] K. Katayama, H. Matsubara, F. Nakanishi, T. Nakamura, H. Doi, A. Saegusa, T. Mitsui, T. Matsuoka, M. Irikura, T. Takebe, S. Nishine, T. Shirakawa, J. Cryst. Growth 214/215 (2000) 1064.
[63] A. Ishibashi, J. Cryst. Growth 159 (1996) 555.
[64] C. Boney, Z. Yu, W.H. Rowland Jr., W.C. Hughes, J.W. Cook Jr., J.F. Schetzina, G. Cantwell, W.C. Harsch, J. Vac. Sci. Technol. B 14 (3) (1996) 2259.